Thermal analysis of an integrated motor drive with a switching cell array power converter

Journal of Physics: Conference Series **2766** (2024) 012033 doi:10.1088/1742-6596/2766/1/012033

Thermal analysis of an integrated motor drive with a switching cell array power converter

M Grespan[1], S Busquets-Monge[2], E Mas de les Valls[2], X Jordà[3], M Raya di Francisco[3] and D Angeli[4]

[1] DISMI - Dipartimento di Scienze e Metodi dell'Ingegneria, Università di Modena e Reggio Emilia, Via Amendola 2, Pad. Buccola, 42122 Reggio Emilia, Italy
[2] Universitat Politècnica de Catalunya, Carrer de Jordi Girona 31, Les Corts, 08034 Barcelona, Spain
[3] Institut de Microelectrònica de Barcelona, Universitat Autònoma de Barcelona, Campus, Carrer dels Tillers, 08193, Barcelona, Spain
[4] Centro Interdipartimentale EN&TECH, Piazzale Europa 1, 42124 Reggio Emilia, Italy

E-mail: mattia.grespan@unimore.it

Abstract. In modern electric propulsion systems the electric motor is tightly integrated with the power converter and control unit. These so called Integrated Motor Drives can allow for vast improvements in efficiency and volume reduction, due to the elimination of redundant electric components, and the shared case and cooling system between the motor and the power converter. The cooling systems used in these applications must be carefully designed as the motor and power electronics components may feature greatly different temperature limits. This work discusses the development of a thermal model for an integrated motor drive composed by a six phase permanent magnet motor with hairpin windings and a switching-cell-array-based multilevel power converter. The system is modelled by means of a lumped parameter thermal network which includes an accurate model of the motor stator and rotor, as well as the arrangement of the power switches on the converter boards. The conductive resistances are simply obtained from geometric data and material properties. Instead, the convective resistances are evaluated by means of empirical models available in the literature and a CFD model for the cooling jacket. The developed model is employed to assess the feasibility of the presented arrangement of motor and power electronics components from the thermal point of view.

1. Introduction

In the field of electric vehicle propulsion, a great research and development effort is aimed at improving the degree of integration between the electric motor and power converter, as this allows for the reduction of the size and weight of the powertrains while improving their efficiency, thanks to the elimination of superfluous electric components. A critical aspect of the integration between motor and power electronics is the thermal management, as the cooling system shared by the two systems must maintain the temperature of each critical component below its safety limit. Mellor *et al.* [1] laid the foundations for the thermal modelling of electric machines, with their approach based on hollow cylindrical elements. Several authors built upon this concept by proposing simplified approaches [2], sensitivity analyses [3], and advanced component-level modelling approaches [4]. In [5] an analogous thermal model for an hairpin winding machine is presented. Reimers *et al.* [6] proposed a thorough review on the design of inverters and their

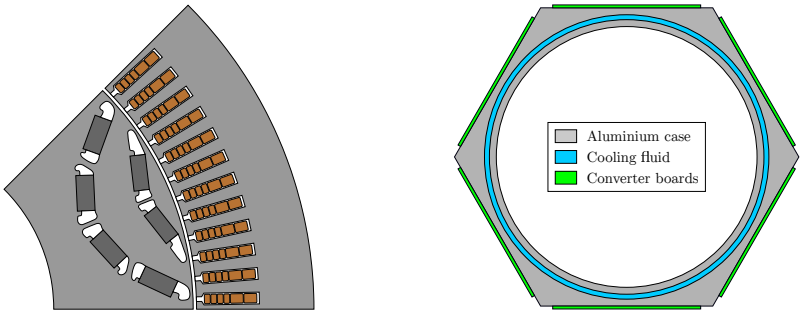

(a) (b)

Figure 1. Cross section of the electric machine [8], with the arrangement of magnets and windings (a), and a schematic of the proposed cooling solution with the six converter legs (b).

cooling systems by presenting examples from commercial automotive applications. This paper discusses the development of a thermal model for an integrated motor drive, aimed at verifying the feasibility of the proposed cooling solution. The overall system is represented by a Lumped Parameter Thermal Network (LPTN) that models in detail the stator and rotor of the electric machine, as well as the power converter and the shared cooling jacket. Conductive resistances are computed from geometric data and material properties. Convective resistances are derived from empirical and CFD models for the air gap and cooling jacket, respectively. The developed numerical tools are used to assess the feasibility of the proposed arrangement from the thermal point of view.

2. Case study

The examined integrated motor drive consists of a six phase permanent magnet synchronous motor and the associated power converter. The electric machine features a six-layer hairpin winding layout with H-class rated insulation, meaning that the maximum allowable winding temperature is 180 °C. The rotor features neodymium-iron-boron magnets with a Curie temperature of 310 °C. Both the stator and rotor laminations are made out of NO20-1200H electrical steel. Figure 1a shows a slice of the motor cross section that highlights the position of the magnets, along with the layout of the windings. The power converter features a multilevel switching cell array architecture [7]. Each converter leg is composed by eight switching cells, each made up of a main power switch and its driver, along with the iFuse, an additional switch used to deactivate the switching cell in case of a fault. These power devices are directly embedded in the PCBs to improve efficiency and reduce the size of the converter legs. The proposed cooling system consists of an hexagonal cooling jacket with the external surfaces serving as cold plates for the inverter PCBs. The cooling channels feature a simple circumferential design with a height of 5 mm and a width of 40 mm. Figure 1b shows a simple schematic of the proposed cooling system where the six converter legs are mounted on the external walls of the cooling jacket.

3. Modelling approach

3.1. System model

The integrated assembly composed by the electric motor, the power converter, and their shared cooling system is modelled by means of a thermal network. The electric motor domain is reduced down to a basic geometry consisting of a stator slot, along with the associated conductors and insulation, and half of the two adjacent teeth. This allows for a vast reduction of the number of nodes included in the thermal model, and furthermore, this basic thermal network

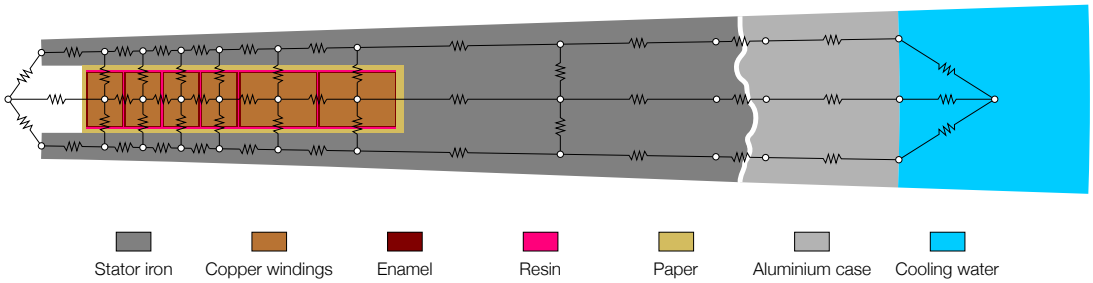

Figure 2. Schematic of the network of thermal resistances used to model the stator of the electric motor, with the main winding and insulation components highlighted.

can be repeated along the circumferential and axial directions to easily extend the computational domain. The stator thermal network is shown in the schematic of figure 2, where the materials making up the stator are clearly highlighted. The conductive thermal resistance between a pair of nodes is evaluated by summing the contributions given by each layer of material:

$$R_{ij} = \sum_k \frac{1}{S_k \, \lambda_k} \, , \tag{1}$$

where S_k and λ_k are the conduction shape factor and thermal conductivity of a single layer, respectively. The shape factors are computed on the basis of geometric data: in the windings, flat plate shape factors are used for the copper busbars and the insulation layers:

$$S_{\mathrm{fp}} = \frac{A}{t} \, , \tag{2}$$

while in the stator magnetic circuit radial and circumferential conduction shape factors are employed; these are computed by means of the general approach proposed by Yovanovich [9]:

$$S_r = \frac{\Delta z \, \Delta \vartheta}{\ln\left(r_e / r_i\right)}, \qquad S_\vartheta = \frac{\Delta z \, \ln\left(r_e / r_i\right)}{\Delta \vartheta} \, . \tag{3}$$

The contact resistances between the stator and the internal wall of the cooling jacket are estimated by assuming conduction through an equivalent air gap, modelled by means of a flat plate shape factor, where the heat transfer area is $A = 2\,\pi\, r_s \, \Delta z$ and equivalent thickness is $t = 0.006\,\mathrm{mm}$, as suggested in [4]. The convective resistances associated with the air gap and cooling jacket are defined as:

$$R_{\mathrm{conv}} = \frac{1}{h\, A} \, , \tag{4}$$

where h is the convective heat transfer coefficient. The h-values in the air gap are obtained from the correlation by Bjorklund and Kays [10] for Taylor-Couette flows, while the ones associated with coolant flow are derived from a dedicated CFD model which will be presented in §3.2. The thermal model of the rotor is obtained by simplifying the geometry presented in figure 1a to represent it in a cylindrical system of reference at a reduced node count. The modified rotor geometry is shown in figure 3 along with its thermal network model. Losses in the stator and rotor magnetic circuits, windings, and magnets are obtained from 2D electromagnetic FE analyses analogous the ones presented in [8] and [11]. The thermal model for the power converter and external wall of the cooling jacket features a much simpler arrangement: all the nodes standing for the main and iFuse switches are connected in parallel to the last copper layer of the

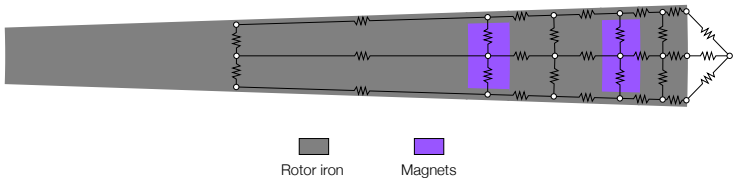

Figure 3. Arrangement of nodes and thermal resistances making up the rotor thermal model.

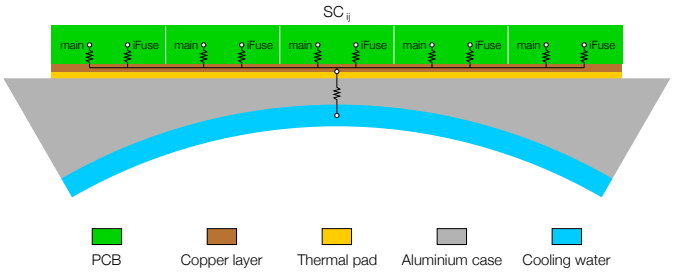

Figure 4. Thermal network model of one of the six converter legs.

PCB via the junction resistance $R_j = 0.5$ °C/W, as shown in figure 4. The PCB is connected to the case by means of a carbon fibre thermal pad. Also in this case convective resistances are obtained from the CFD model presented in §3.2. The switching and conduction losses of each power switch are derived from initial estimates and are omitted here for brevity.

3.2. Cooling jacket model

The heat transfer coefficients associated with the internal and external walls of the cooling jacket are obtained by developing a dedicated CFD model. In an effort to reduce the required computational effort, a reduced domain comprising one sixth of a single channel is analysed under the assumptions of periodic and incompressible flow. The approach used to obtain the periodic flow solution is extensively described in [12], where it was applied to a similar cooling jacket. Figure 5 shows the selected views of the smoothed structured mesh employed for the discretisation of the computational domain, where the channel vents and the fluid and solid regions are clearly highlighted.

4. Results and discussion

4.1. Validation of the motor thermal model

The thermal network modelling the electric motor is validated by performing an initial test and comparing the results with the ones from a Finite Element Analysis performed on exactly the same motor geometry, which is presented in [11]. The boundary conditions related to the reference FEA are reproduced by considering a coolant temperature of 50 °C and an equivalent heat transfer coefficient of 3000 W/(m^2°C) in the cooling jacket. In this case, due to some limitations of the computational tool used for the FE analysis, the stator and rotor are thermally uncoupled. Figure 6a shows the comparison between the temperature values obtained from the LPTN and FE models in the windings and in the stator magnetic circuit, showing an almost perfect agreement between the two models. This confirms the validity of the modelling approach selected for the electric motor; furthermore, it demonstrates that a model consisting of a small number of thermal resistances can produce the same results as models with a much larger number of degrees of freedom, for this particular motor.

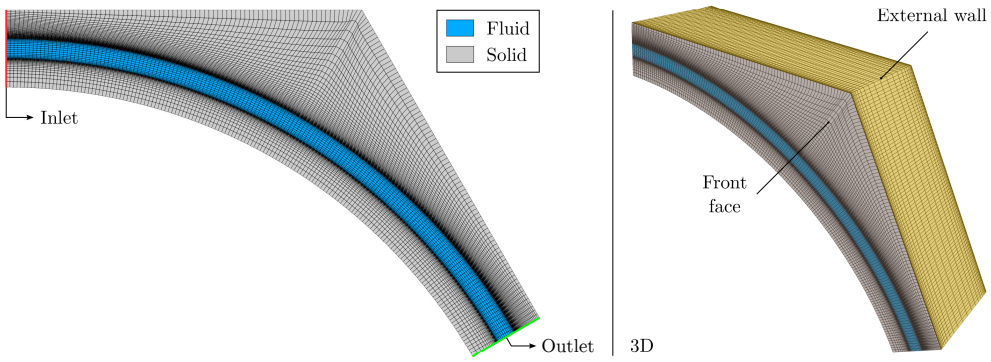

Figure 5. Side and 3D views of the cooling jacket computational mesh, where the inlet, outlet, and the fluid and solid regions are clearly identified.

4.2. Cooling jacket
Figure 6b shows colourmaps of dimensionless velocity magnitude and temperature difference $\Delta T^* = (\overline{T}_{\mathrm{w}} - T)/(\overline{T}_{\mathrm{w}} - \overline{T}_{\mathrm{b}})$, that are obtained on centred transversal sections of the cooling jacket. As expected, the velocity profile is not symmetric with respect to the channel centreline due to the effect of centrifugal forces. The heat transfer effectiveness related to the internal and external walls is evaluated by means of an equivalent Nusselt number, which is computed as:

$$\mathrm{Nu} = \frac{q'' \, y}{\lambda \, (\overline{T}_{\mathrm{w}} - \overline{T}_{\mathrm{b}})} \, , \tag{5}$$

where $\overline{T}_{\mathrm{w}}$ and $\overline{T}_{\mathrm{b}}$ are the mean wall and fluid bulk temperatures, respectively. y is the channel height, which is chosen as the reference length of the problem. In the case of a flow of a 50% by mass solution of water and ethylene glycol at 5 l/min, the Nusselt number values related to the inner and outer walls are 21.5 and 19.4, respectively.

4.3. System level results
The feasibility of the proposed motor and converter architecture, along with the shared cooling system, is assessed by comparing the temperature values of the main components with their respective thermal limit, assuming a mean coolant bulk temperature of 80 °C. As can be seen in table 1, the presented cooling system is able to guarantee the safe and correct operation of the main components constituting the integrated motor drive. On the motor side, the innermost magnets are the limiting factor from the thermal point of view, as they feature the highest temperature due to the large equivalent resistance to the coolant; furthermore, large safety margins must be maintained in case of the magnets, as localised hot spots could lead to the partial demagnetisation of the magnets, which would significantly reduce the motor performance.

5. Conclusions
This work discussed the development of a basic model for the thermal analysis of an integrated motor drive, with the aim of assessing the effectiveness of its cooling system. The examined motor drive consisted of a six phase permanent magnet motor and a switching-cell-array-based multilevel power converter. The integrated assembly, along with its cooling system, was modelled by means of a lumped parameter thermal network. The thermal resistances were obtained from geometrical parameters, empirical models, and a dedicated CFD model for the cooling jacket. The numerically obtained heat transfer coefficients were employed, along with the thermal

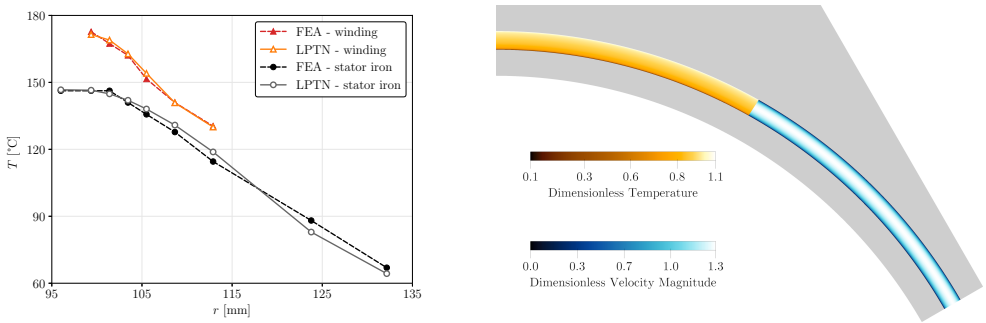

(a) (b)

Figure 6. Comparison between the temperature values of the windings and stator iron obtained from the LPTN and FE models (a). Colourmaps of dimensionless velocity magnitude and temperature difference on a transversal cross section of the cooling jacket (b).

network model, to verify the effectiveness of the proposed cooling concept. The initial results proved to be promising, as the proposed layout appears to provide sufficient cooling for all the major components. Future research activity will be aimed at the expansion of the model along the axial direction of the motor, to include the end-winding losses and to compute the coolant temperature increase along the cooling jacket.

Table 1. Temperature limits and numerically obtained maximum temperature values of the main components of the integrated motor drive.

Component	Temperature limit [°C]	T [°C]	$T - T_{\text{ref}}$ [°C]
Windings	180	127	47
Magnets	310	196	116
Converter	200	118	38

Acknowledgements
This work was funded by the European Union's Horizon Europe research and innovation program under grant agreement No. 101056781. Views and opinions expressed are however those of the authors only and do not necessarily reflect those of the European Union or CINEA. Neither the European Union nor the granting authority can be held responsible for them.

References
[1] Mellor P H, Roberts D and Turner D 1991 *IEE Proc. Electr. Power Appl.* **138**(5) 205–218(13)
[2] Boglietti A, Cavagnino A, Lazzari M and Pastorelli A 2002 *Conf. Rec. Ind. Appl. Soc.* vol 2 pp 723–730
[3] Boglietti A, Cavagnino A and Staton D 2004 *Conf. Rec. Ind. Appl. Soc.* vol 4 pp 2469–2476
[4] Staton D, Boglietti A and Cavagnino A 2005 *IEEE Trans. Energy Convers.* **20** 620–628
[5] Zhang *et al.* 2021 *IEEE Trans. Transp. Electrif.* **7** 2914–2926
[6] Reimers J, Dorn-Gomba L, Mak C and Emadi A 2019 *IEEE Trans. Veh. Technol.* **68** 3337–3350
[7] Busquets-Monge S and Caballero L 2019 *IEEE Trans. Ind. Electron.* **66** 25–36
[8] Pastura M, Notari R, Nuzzo S, Barater D and Franceschini G 2023 *IEEE Trans. Transp. Electrif.* 1–1
[9] Yovanovich M 1973 *11th Aerosp. Sci. Meet.*
[10] Bjorklund I S and Kays W M 1959 *J. Heat Transfer* **81** 175–183 ISSN 0022-1481
[11] Pastura M 2023 *PhD thesis - Alma Mater Studiorum - University of Bologna*
[12] Grespan M, Campanelli L, Angeli D and Freddi R 2024 *J. Phys. Conf. Ser.* **2685** 012016